

10-2013

## Suspended Lipid Bilayer For Optical And Electrical Measurements Of Single Ion Channel Proteins

Suneth P. Rajapaksha

Xuefei Wang

H. Peter Lu

*Bowling Green State University*, [hplu@bgsu.edu](mailto:hplu@bgsu.edu)

Follow this and additional works at: [https://scholarworks.bgsu.edu/chem\\_pub](https://scholarworks.bgsu.edu/chem_pub)

 Part of the [Chemistry Commons](#)

---

### Repository Citation

Rajapaksha, Suneth P.; Wang, Xuefei; and Lu, H. Peter, "Suspended Lipid Bilayer For Optical And Electrical Measurements Of Single Ion Channel Proteins" (2013). *Chemistry Faculty Publications*. 76.  
[https://scholarworks.bgsu.edu/chem\\_pub/76](https://scholarworks.bgsu.edu/chem_pub/76)

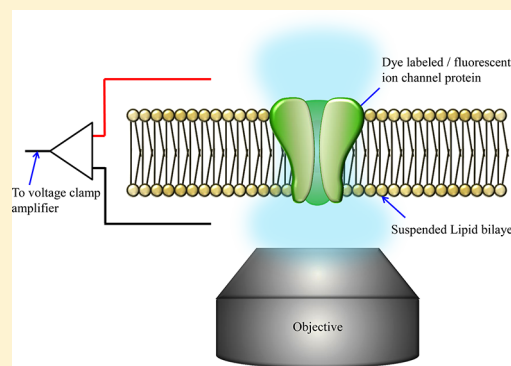
This Article is brought to you for free and open access by the Chemistry at ScholarWorks@BGSU. It has been accepted for inclusion in Chemistry Faculty Publications by an authorized administrator of ScholarWorks@BGSU.

# Suspended Lipid Bilayer for Optical and Electrical Measurements of Single Ion Channel Proteins

Suneth P. Rajapaksha, Xuefei Wang, and H. Peter Lu\*

Department of Chemistry and Center for Photochemical Sciences, Bowling Green State University, Bowling Green, Ohio 43403, United States

**ABSTRACT:** Making and holding an artificial lipid bilayer horizontally in an aqueous solution within the microscopic working distance of  $\sim 100\ \mu\text{m}$  are essential for simultaneous single molecule imaging and single ion-channel electrical current recording. However, preparation of such a lipid bilayer without a solid support is technically challenging. In a typical supported lipid bilayer, the asymmetric local environments and the strong perturbation of the underneath solid or dense surface can diverge the normal behavior of membrane proteins and lipids. On the other hand, the suspended lipid bilayers can provide a native local environment for the membrane proteins and lipids by having fluids on both sides. In this technical report, we present a simple and novel methodology for making a suspended lipid bilayer that can be used for recording the single-molecule diffusion and single ion-channel electrical measurements of ion-channel proteins. Our approach has a higher validity for studying the molecular diffusions and conformational fluctuations of membrane proteins without having perturbations from supporting layers. We demonstrate the feasibility of such an approach on simultaneous single-molecule fluorescence imaging and electric current measurements of ion channel proteins.



Membrane proteins are proven to be vital in many cellular processes, including cell polarity, membrane transportation, and cell signaling.<sup>1–3</sup> However, their dynamic properties have not been studied as extensively as water-soluble proteins due to the complexity of membrane sample preparation and characterization. Two experimental approaches are widely used to study the dynamics of the membrane proteins, especially ion channels, at the single-molecular level: single-molecule fluorescence imaging and single ion-channel electrical current recording. Both methods are sensitive to intrinsic molecular conformational changes relative to local environment fluctuations in real time and describe the ion channels in complementary perspectives, such as the channel activity dynamics, protein diffusion dynamics, and protein conformational dynamics.

Combining single-molecule fluorescence spectroscopy with conventional but powerful single ion-channel electrical current measurements has been continuously reported since 1999.<sup>4–15</sup> For example, Yanagida and co-workers reported single-channel fluorescence images acquired from total internal reflection fluorescence microscopy (TIRFM) correlated with single-channel current measurement for Cy3-labeled alamethicin molecules.<sup>6</sup> Lu and co-workers demonstrated simultaneous patch-clamp electrical current measurement correlated with single-molecule FRET imaging and single-molecule ultrafast spectroscopy.<sup>4,5,7,13,14</sup> Woolley and Schutz demonstrated a simultaneous optical and electrical recording of single gramicidin channels in a lipid bilayer on a micropinhole.<sup>16</sup> Wallace et al. developed planar lipid bilayers between an aqueous droplet and a hydrogel support immersed in a lipid–oil solution to probe ion

channels optically and electrically.<sup>17–19</sup> Further, there are significant advancements in correlating fluorescence imaging with whole cell ion-channel electrical current measurement.<sup>9–12</sup> Although not mentioned in this brief report, many advancements in combining fluorescence imaging and electric recording can be found in recent literature.

Nevertheless, one of the technical bottlenecks to achieve a combined electrical current recording and fluorescence microscopic imaging of ion-channel proteins is to develop a suspended lipid bilayer within the microscopic imaging distance, which has not been demonstrated previously to the best of our knowledge. Most attempts made earlier to combine fluorescence imaging and ion channel current recording were performed on supported lipid bilayers.<sup>6,20</sup> The supported bilayers provide complex experimental environments, such as (1) the solid/gel support does not provide the necessary free solution phase for positioning an electrode and (2) they may perturb the behaviors of membrane proteins,<sup>21,22</sup> impacting the diffusion dynamics and conformational dynamics. There were demonstrations using a patch-clamp glass-pipet aperture to hold a small size lipid bilayer; however, it can complicate the fluorescence imaging by high light-scattering background from the glass wall.<sup>4,5,7,13,14</sup> These technical barriers more than often make the analysis of ion channel dynamics complex in terms of identifying the artifact of sample handling versus the intrinsic protein dynamics.

Received: May 3, 2013

Accepted: August 31, 2013

Published: August 31, 2013

Conversely, the artificial lipid bilayer experiment can be conducted resembling the real biological cell membrane by using the suspended lipid bilayers in the solution, and if the bilayer is large enough, it avoids laser light scattering when the bilayer is illuminated with a focused laser light. We have developed an apparatus to prepare such a lipid bilayer assembly to facilitate the combined single molecule fluorescence imaging and single ion-channel electrical current recording. We have used fluorescein-tagged colicin Ia,<sup>23–29</sup> a voltage-gated single-subunit ion-channel protein, as a model system to demonstrate the simultaneous single-molecule fluorescence imaging and single ion-channel current recording on the suspended lipid bilayers. Colicin Ia is one of the non-neuronic ion channel proteins being produced by certain strains of *Escherichia coli* to kill the other sensitive strains of *E. coli* lacking the specific immunity protein.<sup>23</sup> Colicin Ia consists three domains: amino terminal T-domain, central R-domain, and carboxy terminal C-domain. The C-domain contains ten  $\alpha$ -helices which are responsible for forming ion channels across the biological membrane.<sup>24–26</sup> Some helices of the C-domain move across the lipid bilayer to the trans side at the presence of a voltage gradient forming a channel across the membrane.

In this report, we discuss the development of a suspended lipid bilayer to combine the single molecule imaging and single ion-channel electric current recording, which are demonstrated here by using colicin Ia ion channel.

## MATERIALS AND METHODS

1,2-diphytanoyl-*sn*-glycero-3-phosphocholine (DPhPC) was purchased from Avanti Polar Lipids Inc. (Alabaster, Alabama). KCl, NaOH, HCl, and HEPES (Aldrich) were used as received. The colicin Ia used in our experiments was purified, mutated, fluorescein-labeled, and biotinylated<sup>30</sup> by Prof. A. Finkelstein's group in Albert Einstein College of Medicine, NY, and only has the C-domain (the term "colicin Ia" in the materials and methods and the results and discussion sections refers to the C-domain of colicin Ia). The fluorescein and the biotin were labeled on the protein at the 511 amino acid position and at the 594 amino acid position, respectively.

**The Bilayer Apparatus.** The components of the apparatus that were used to prepare the suspended artificial lipid bilayer are shown in Figure 1. Namely, (a) 24 × 60 mm cover glass (GoldSeal, EMS, Hatfield, PA). (b) Double-sided tape that is smaller than the size of the cover glass (Scotch brand tapes, 3M, MN). (c) Plastic transparent sheet with three holes where the central hole was created on a micrometer scale. We have investigated both Teflon films and plastic transparent sheets for preparing the lipid bilayers and did not identify any significant advantage of Teflon films over transparent sheets. Hence, we used transparent sheets due to handling simplicity. (d) Three pieces of 1/4" PVC tubes (VWR LabShop, Batavia, IL). The cover glass was first washed with hexane, then dipped in acetone to sonicate for about 10–20 min before being rinsed with tap water for several times and finally with the deionized water. The rectangular piece of the tape was removed to make a confined space between the cover glass and plastic transparent sheet, connecting the three compartments of the final apparatus (Figure 1b). The plastic transparent film (smaller than the size of the cover glass, approximate sizes are indicated in the Figure 1) was pierced at the center with a sharp needle, and then the extrusions on the opposite side were shaved with a sharp blade to have a smooth, circular hole with a diameter of 50–200  $\mu\text{m}$ . Two other apertures were made as displayed in triangular shapes in

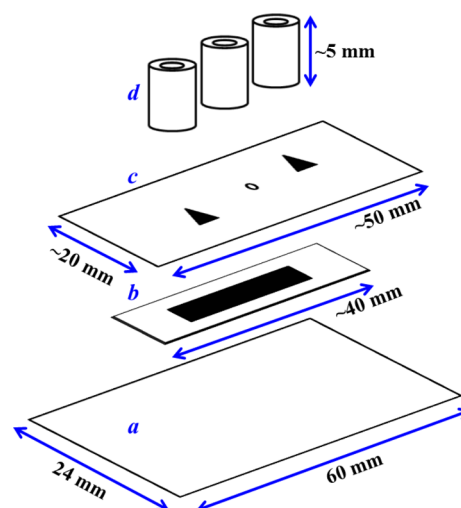


**Figure 1.** The bilayer apparatus with (a) a 24 × 60 mm cover glass, (b) double-sided tape, (c) a plastic transparent sheet with three holes, and (d) three small PVC tubes.

Figure 1c. Then the plastic film was pasted on the cover glass with the help of the double-sided tape, ensuring that all the three holes were inside the removed rectangular space of the double-sided tape. The PVC tubes, each ~0.5 cm in height, were pasted on the holes of the plastic film to create three compartments.

**Lipid Bilayer Preparation.** The bilayer was prepared by painting 10–20 mg/mL of 1,2-diphytanoyl-*sn*-glycero-3-phosphocholine, DPhPC in *n*-decane solution across the aperture of the central chamber. The lipid bilayer formed across the aperture of the central chamber is shown in Figure 2A, and the procedure for making the lipid bilayer is listed: (1) the electrolyte solution (1 M KCl, 5 mM CaCl<sub>2</sub>, 1 mM EDTA, 20 mM HEPES buffer, pH = 8.0)<sup>31</sup> was filled in all three chambers, and the space between the cover glass and the plastic film of the apparatus which is confined by the double-sided tape. (2) The lipid solution was painted on the central hole by using a heat-flattened capillary tube (diameter 0.69 mm, Drummond Scientific Company, Broomall, PA). The membrane formed across the aperture spontaneously thinned into bilayer configuration due to the plateau Gibbs boarder and London–van der Waals forces.<sup>32,33</sup> Further, the plateau Gibbs border helps the lipid bilayer to stay in an unstretched condition without changing the membrane tension significantly under a certain hydrostatic pressure gradient.<sup>34</sup> It was microscopically identified that the lipid bilayer is always formed close to the lower edge of the transparent sheet by having same focal distance ( $f_0$ ) for the lower surface of the transparent sheet and the lipid bilayer as shown in Figure 2B. The lipid bilayer was identified by (i) the specific capacitance value that is in agreement with the typical lipid bilayer capacitance of 0.8–1.0  $\mu\text{F}/\text{cm}^2$  and (ii) the microscopic observation of the lipid bilayer thinning process.

**Single Ion-Channel Fluorescence Imaging and Electric Current Measurements.** The experimental setup is illustrated in Figure 2C. The bilayer was illuminated with a 488 nm laser beam (Argon ion laser, Melles Griot, Carlsbad, CA) at a mean intensity of ~0.30  $\text{kW}/\text{cm}^2$  in a wide-field epifluorescence mode. The incident laser beam was directed to the objective through an aperture and reflected by a dichroic mirror (Z488RDC, DM in Figure 2D, Chroma Technology Corp., Montpelier, VT). The fluorescence signals were collected with an inverted microscope (Axiovert 200M, Zeiss) equipped with a 60× objective (OBJ)

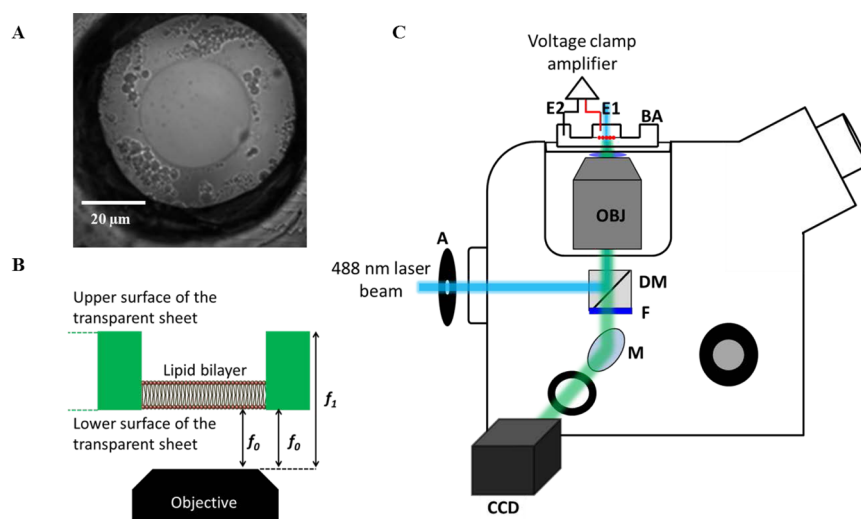


**Figure 2.** (A) An image of the suspended lipid bilayer. (B) The location of the suspended lipid bilayer in the transparent sheet. The lipid bilayer and the lower surface of the transparent sheet have the same focal length ( $f_o$ ), and the upper surface of the transparent sheet has a higher focal length ( $f_i$ ). (C) Schematic of simultaneous single ion-channel optical and electric current recording system. A, aperture; DM, dichroic mirror; F, filter; M, reflection mirror; OBJ, objective; BA, bilayer apparatus; and E1 and E2, electrodes.

(N.A. = 1.20). The collected photons from the sample were filtered with a HQ50SLP filter (F in Figure 2D, Chroma Technology Corp.) and recorded with a liquid-nitrogen-cooled CCD camera (Princeton Instrument, Trenton, NJ). The single molecule images were collected with 50 ms exposure time and 50 ms delay time.

All the single ion-channel electric current measurements were conducted using EPC7 plus patch clamp amplifier (HEKA Elektronik Dr. Schulze GmbH) and filtered at 1 kHz. The data were recorded using LIH1600 acquisition interface and PULSE V8.80. The presence of a single-ion channel on the lipid bilayer was confirmed by the typical single channel open–close activity.<sup>35,36</sup>

## RESULTS AND DISCUSSION

We have recorded diffusion trajectories and single-ion-channel current trajectories of fluorescein-labeled colicin Ia (Figure 3) by adding five microliters of low concentration ( $\sim 1 \times 10^{-9}$  M) protein solution to the cis side of the suspended membrane and allowing it to insert in the membrane. Some of the recorded optical and electrical current trajectories are shown in Figure 3 to demonstrate the capability of our suspended lipid bilayer for hosting membrane ion channel proteins. Figure 3A shows two-dimensional diffusion trajectories of colicin Ia on the suspended lipid bilayer over a 5 s time period. Figure 3B shows two trajectories of single ion-channel electric current open–close fluctuation recorded under the same sample condition. These measurements confirm the stability of our lipid bilayer for a considerably long time for recording long diffusion and ion-channel electric current trajectories.

Figure 4A shows a 2D diffusion trajectory colicin Ia for a 4 s time period. Each position coordinate in the trajectory is determined from an imaging frame with a 50 ms exposure time and a 50 ms delay time. The mean square displacement (MSD) of the two-dimensional diffusion is calculated by using eq 1.<sup>37–41</sup>

$$\text{MSD} = \langle r_{(\Delta t)}^2 \rangle = \langle (x_{(t+\Delta t)} - x_{(t)})^2 + (y_{(t+\Delta t)} - y_{(t)})^2 \rangle \quad (1)$$

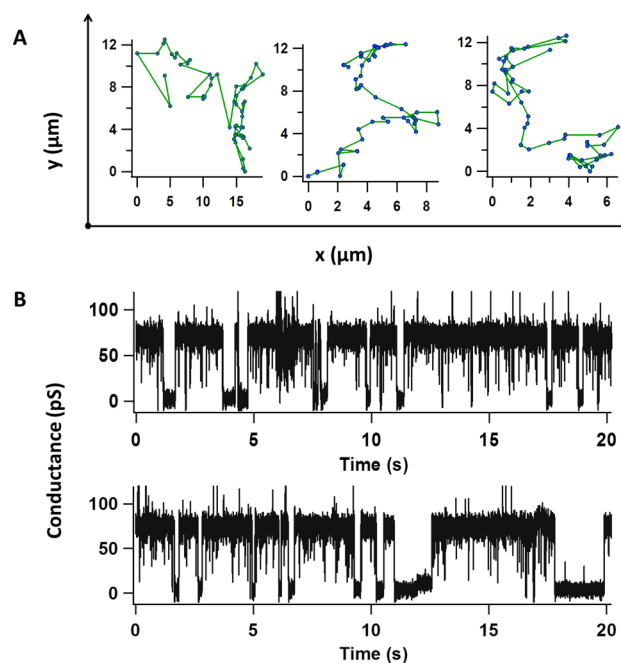


**Figure 3.** Diffusion and single ion channel current trajectories of colicin Ia on the suspended lipid bilayer. (A) Two dimensional diffusions of colicin Ia on the lipid bilayer. Each trajectory is 5s long and recorded with 50 ms exposure time and 50 ms delay time. (B) 20 s Long single-ion-channel conductance trajectories of colicin Ia at a 70 mV transmembrane voltage.

Where,  $x_{(t)}$  and  $y_{(t)}$  are  $x$  and  $y$  coordinates of the fluorescein-labeled colicin Ia at time  $t$ .  $x_{(t+\Delta t)}$  and  $y_{(t+\Delta t)}$  denotes the coordinates of colicin Ia after  $\Delta t$  time. Figure 4B shows the MSD as a function of time lag and that indicates the directed motion of the colicin Ia in the suspended lipid bilayer.<sup>39,42,43</sup> The directed motion is a combination of the molecular diffusion and the drift on a certain direction. The analytical form of the directed motion is given by eq 2.<sup>41–43</sup>

$$\langle r^2 \rangle = 4Dt + V^2t^2 \quad (2)$$

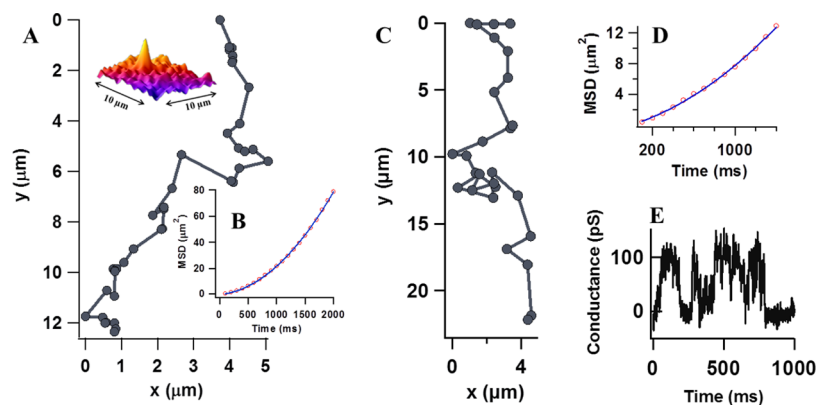


**Figure 4.** (A) 2D diffusion trajectory of colicin Ia on the artificial suspended lipid bilayer recorded over 4s. The inset shows the single-molecule image of the fluorescein-tagged colicin Ia on the horizontal lipid bilayer. (B) MSD of the trajectory shown in Figure 4A as a function of time lag. Diffusion coefficient and velocity of the trajectory are calculated by fitting with eq 2 to be  $9.77 \times 10^{-9} \text{ cm}^2/\text{s}$  and  $4.17 \times 10^{-4} \text{ cm/s}$ , respectively. (C) The 2D diffusion of colicin Ia on the suspended lipid bilayer over 2.7 s, which is recorded simultaneously with the conductance trajectory shown in Figure 4E. (D) MSD from the trajectory shown in Figure 4C as a function of time lag, with  $D$  and  $V$  for the motion as  $11.65 \times 10^{-9} \text{ cm}^2/\text{s}$  and  $1.73 \times 10^{-4} \text{ cm/s}$ , respectively. (E) A single-ion-channel conductance trajectory recorded at 70 mV.

Where  $D$  is the diffusion coefficient,  $V$  is the velocity of the motion, and  $t$  is the time lag.  $D$  and  $V$  for the diffusion of colicin Ia on the horizontal unsupported lipid bilayer are calculated as  $3.93 \pm 1.81 \times 10^{-9} \text{ cm}^2/\text{s}$  and  $1.02 \pm 0.48 \times 10^{-4} \text{ cm/s}$ , respectively, as averaged results from calculations of 14 fluorescence imaging trajectories. The drifting velocity is  $\sim 1 \text{ nm/ms}$ . For a 50 ms imaging recording time, the average drifting distance is comparable to the optical diffraction limit spatial resolution of  $\sim 250 \text{ nm}$  diameter. The drift diffusive motions are most likely due to the lipid bilayer dynamics under the support free and buffer solution local environment. Undoubtedly, the motion of the protein has a strong correlation with the surrounding lipids and their hydrated radii, which ultimately decide the averaged positioning coordinates of the protein in the lipid bilayer. Our measured diffusion coefficient of colicin Ia is consistent with the published similar protein diffusion coefficients in the lipid bilayers.<sup>44–46</sup> It is well-demonstrated in the literature that the diffusion coefficient has a strong correlation with the size of the proteins.<sup>47</sup> Furthermore, the magnitude of the coefficient can be dependent on the number of  $\alpha$ -helices that are inserted in the lipid membrane. For example, bacteriorhodopsin with seven transmembrane helices diffuses at  $8 \times 10^{-10} \text{ cm}^2/\text{s}$  in the membrane, about 3.8 times slower than the single helix  $L_{18}$  peptide ( $3.1 \times 10^{-9} \text{ cm}^2/\text{s}$ ).<sup>47</sup> Similarly, colicin Ia, nevertheless showing essentially consistent diffusion coefficients compared to that of the other proteins reported in the literature,<sup>10,47–49</sup> can have different diffusion coefficients, depending on the number of transmembrane helices inserted in the lipid membrane. The single-ion-channel conductance for colicin Ia is calculated by using the population distribution of the conductance as  $70 \pm 5 \text{ pS}$  in the suspended lipid bilayer at a 70 mV transmembrane voltage.

The primary advantage of the suspended lipid bilayer is its capability of recording simultaneous single-molecule fluorescence images and single ion-channel current fluctuations, besides the intrinsic advantage of holding the lipid bilayer in an unperturbed solution local environment, more closely resembling the cell membrane than the traditional lipid bilayer with a solid surface support does. Figure 4 (panels C and E) shows a typical simultaneously recorded optical and ion-channel current measurements of colicin Ia in the suspended lipid bilayer. The single-ion-channel electric current trajectory is shown in Figure 4E and the single ion-channel conductance is calculated as 88 pS

at a 70 mV cross-membrane voltage. Our measured values of the single-ion-channel conductance of colicin Ia are in agreement with the reported values (60–120 pS), confirming the normal channel structure of colicin Ia in the suspended lipid bilayer.<sup>23</sup>

It is interesting to observe that the diffusions of colicin Ia suspended the lipid bilayer as a directed motion in each trajectory. Though this type of nonlinear relationships of MSD with time is common in biological systems, it is difficult to identify the exact reason for the drifting in the systems like artificial lipid bilayers. Most probably, the motion of colicin Ia is associated with the motion of the entire lipid bilayer where the bilayer is acting as a dynamic fluid. When the fluid is moving to a certain direction due to its hydrodynamic nature, the protein is also moving in the same direction as that of lipids, while showing the Brownian type motion. However, further understanding is necessary for comprehensively describing the motion of colicin Ia on the artificial suspended lipid bilayers.

## CONCLUSION

We have developed and demonstrated a suspended lipid bilayer for studying protein diffusion in lipid bilayers and for simultaneous recording of optical imaging and the electrical current recording of membrane ion-channel proteins, enabling studies of ion-channel proteins in an unperturbed lipid environment. We used the fluorescein-tagged colicin Ia as the membrane ion-channel protein to demonstrate the capability of the lipid bilayer for simultaneous measurements. Most importantly, this lipid bilayer provides a close native and unperturbed local environment to the membrane lipids and membrane proteins than other types of artificially formed lipid bilayers for microscopic imaging experiments. Our new approach provides a new platform to perform simultaneous optical imaging and single ion-channel electrical recording of membrane ion-channel proteins.

## AUTHOR INFORMATION

### Corresponding Author

\*E-mail: hplu@bgsu.edu. Tel: 419-372-1840.

### Notes

The authors declare no competing financial interest.

## ACKNOWLEDGMENTS

We acknowledge the support of this work from the Ohio Eminent Scholar Endowment and NIH/NIGMS. We acknowledge the contribution of Dr. Somes Das on the technical development of making the unsupported lipid bilayer in the early stage of this project. We also acknowledge Prof. A. Finkelstein from the Albert Einstein College of Medicine to provide us the colicin Ia used in our demonstration and experiments.

## REFERENCES

- (1) Lenaz, G. *Bioscience Reports* **1987**, *7*, 823–837.
- (2) Hille, B. *Ion Channels of Excitable Membranes*, 3rd ed.; Sinauer Associates, Inc.: Sunderland, MA, 2001.
- (3) Sakmann, B.; Neher, E. *Single Channel Recordings*; Plenum Press: New York, 1995.
- (4) Harms, G. S.; Orr, G.; Montal, M.; Thrall, B. D.; Colson, S. D.; Lu, H. P. *Biophys. J.* **2003**, *85*, 1826–1838.
- (5) Harms, G.; Orr, G.; Lu, H. P. *Appl. Phys. Lett.* **2004**, *84*, 1792–1794.
- (6) Ide, T.; Yanagida, T. *Biochem. Biophys. Res. Commun.* **1999**, *265*, 595–599.
- (7) Orr, G.; Montal, M.; Thrall, B. D.; Colson, S. D.; Lu, H. P. *Biophys. J.* **2001**, *80*, 151a.
- (8) Borisenko, S. V.; Kordyuk, A. A.; Kim, T. K.; Koitzsh, A.; Knupfer, M.; Fink, J.; Golden, M. S.; Eschrig, M.; Berger, H.; Follath, Y. *Phys. Rev. Lett.* **2003**, *90*, 207001.
- (9) Sonnleitner, A.; Mannuzzu, L. M.; Terakawa, S.; Isacoff, E. Y. *Proc. Natl. Acad. Sci. U.S.A.* **2002**, *99*, 12759–12764.
- (10) Harms, G. S.; Cognet, L.; Lommerse, P. H. M.; Blab, G. A.; Kahr, H.; Gamsjäger, R.; Spaink, H. P.; Soldatov, N. M.; Romanin, C.; Schmidt, T. *Biophys. J.* **2001**, *81*, 2639–2646.
- (11) Zheng, J.; Zagotta, W. N. *Neuron* **2000**, *28*, 369–374.
- (12) Demuro, A.; Parker, I. *Biol. Res.* **2004**, *37*, 675–679.
- (13) Orr, G.; Harms, G.; Thrall, B. D.; Montal, M.; Colson, S. D.; Lu, H. P. *Biophys. J.* **2002**, *82*, 255a.
- (14) Lu, H. P. *Acc. Chem. Res.* **2005**, *38*, 557–565.
- (15) Loughheed, T.; Borisenko, S.; Hand, C. E.; Woolley, G. A. *Bioconjugate Chem.* **2001**, *12*, 594–602.
- (16) Borisenko, S.; Loughheed, T.; Hesse, J.; Füreder-Kitzmüller, E.; Fertig, N.; Behrends, J. C.; Woolley, G. A.; Schütz, G. J. *Biophys. J.* **2003**, *84*, 612–622.
- (17) Heron, A. J.; Thompson, J. R.; Mason, A. E.; Wallace, M. I. *J. Am. Chem. Soc.* **2007**, *129*, 16042–16047.
- (18) Heron, A. J.; Thompson, J. R.; Cronin, B.; Bayley, H.; Wallace, M. I. *J. Am. Chem. Soc.* **2009**, *131*, 1652–1653.
- (19) Harriss, L. M.; Cronin, B.; Thompson, J. R.; Wallace, M. I. *J. Am. Chem. Soc.* **2011**, *133*, 14507–14509.
- (20) Ide, T.; Ichikawa, T. *Biosens. Bioelectron.* **2005**, *21*, 672–677.
- (21) Hetzer, M.; Heinz, S.; Grage, S.; Bayerl, T. M. *Langmuir* **1998**, *14*, 982–984.
- (22) Feng, Z. V.; Spurlin, T. A.; Gewirth, A. A. *Biophys. J.* **2005**, *88*, 2154–2164.
- (23) Jakes, K. S.; Kienker, P. K.; Finkelstein, A. Q. *Rev. Biophys.* **1999**, *32*, 189–205.
- (24) Weiner, M.; Freymann, D.; Ghosh, P.; Stroud, R. *Nature* **1997**, *385*, 461–464.
- (25) Nogueira, R. A.; Varanda, W. A. *J. Membr. Biol.* **1988**, *105*, 143–153.
- (26) Ghosh, P.; Mel, S. F.; Stroud, R. J. *Membr. Biol.* **1993**, *134*, 85–92.
- (27) Kienker, P. K.; Qiu, X.; Slatin, S. L.; Finkelstein, A.; Jakes, K. S. *J. Membr. Biol.* **1997**, *157*, 27–37.
- (28) Slatin, S. L.; Qiu, X.; Jakes, K. S.; Finkelstein, A. *Nature* **1994**, *371*, 158–161.
- (29) Qiu, X.; Jakes, K. S.; Kienker, P. K.; Finkelstein, A.; Slatin, S. L. *J. Gen. Physiol.* **1996**, *107*, 313–328.
- (30) Qiu, X.; Jakes, K. S.; Finkelstein, A.; Slatin, S. L. *J. Biol. Chem.* **1994**, *269*, 7483–7488.
- (31) Kienker, P. K.; Jakes, K. S.; Finkelstein, A. J. *Gen. Physiol.* **2000**, *116*, 587–597.
- (32) Mysels, K. J.; Shinoda, K.; Frankel, S. *Soap Films: Studies of Their Thinning*; Pergamon Press, Inc.: New York, 1959.
- (33) White, S. H. *Biophys. J.* **1970**, *10*, 1127–1148.
- (34) Sachs, F.; Morris, C. *Rev. Physiol., Biochem. Pharmacol.* **1998**, *132*, 1–77.
- (35) O'Connell, A. M.; Koeppe, R. E.; Andersen, O. S. *Science* **1990**, *250*, 1256–1259.
- (36) Sawyer, D. B.; Koeppe, R. E.; Andersen, O. S. *Biochemistry* **1989**, *28*, 6571–6583.
- (37) Matsuoka, S.; Shibata, T.; Ueda, M. *Biophys. J.* **2009**, *97*, 1115–1124.
- (38) Murcia, M. J.; Garg, S.; Naumann, C. *Methods Mol. Biol.* **2007**, *400*, 277–294.
- (39) Saxton, M. J. *Biophys. J.* **1993**, *64*, 1766–1780.
- (40) Fujiwara, T.; Ritchie, K.; Murakoshi, H.; Jacobson, K.; Kusumi, A. *J. Cell Biol.* **2002**, *157*, 1071–1081.
- (41) Kusumi, A.; Sako, Y.; Yamamoto, M. *Biophys. J.* **1993**, *65*, 2021–2040.
- (42) Qian, H.; Sheetz, M. P.; Elson, E. L. *Biophys. J.* **1991**, *60*, 910–921.
- (43) Saxton, M. J.; Jacobson, K. *Annu. Rev. Biophys. Biomol. Struct.* **1997**, *26*, 373–399.
- (44) Schmidt, T.; Schutz, G. J.; Baumgartner, W.; Gruber, H. J.; Schindler, H. *Proc. Natl. Acad. Sci. U.S.A.* **1996**, *93*, 2926–2929.
- (45) Jacobson, K.; Ishihara, A.; Inman, R. *Annu. Rev. Physiol.* **1987**, *49*, 163–175.
- (46) Zhang, F.; Crise, B.; Su, B.; Hou, Y.; Rose, J. K.; Bothwell, A.; Jacobson, K. J. *Cell Biol.* **1991**, *115*, 75–84.
- (47) Gambin, Y.; Lopez-Esparza, R.; Reffay, M.; Sierrecki, E.; Gov, N. S.; Hodges, R. S.; Urbach, W. *Proc. Natl. Acad. Sci. U.S.A.* **2006**, *103*, 2098–2102.
- (48) Koppel, D. E.; Sheetz, M. P.; Schindler, M. *Proc. Natl. Acad. Sci. U.S.A.* **1981**, *78*, 3576–3580.
- (49) Pluen, A.; Netti, P. A.; Jain, R. K.; Berk, D. A. *Biophys. J.* **1999**, *77*, 542–552.